Overcoming repetition rate limitations in liquid crystal laser systems

Research Article | Vol. 26, No. 20 | 1 Oct 2018 | OPTICS EXPRESS 26544
Optics EXPRESS

Overcoming repetition rate limitations in liquid crystal laser systems

MARGARET C. NORMAND,[1] PEIGANG CHEN,[1] CHI CAN,[2] AND PHILIP J. W. HANDS[1,*]

[1]*Institute for Integrated Micro and Nano Systems, School of Engineering, University of Edinburgh, Edinburgh EH9 3FF, UK*
[2]*Holoxica Ltd, Argyle House, 3 Lady Lawson Street, Edinburgh EH3 9DR, UK*
** philip.hands@ed.ac.uk*

Abstract: Liquid crystal lasers have advantageous features, including continuous wavelength tuning at low cost. Although many potential applications have been highlighted, use of these lasers is not widespread, partially due to performance limitations. This paper presents a method of overcoming repetition rate limitations. A rapidly spinning stage is used to allow operation of a LC laser at 10 kHz: two orders of magnitude greater than possible with a static cell. Average power outputs of up to 3.5 mW are achieved along with an improvement in emission stability. Lastly, a mechanical wavelength-switching method is demonstrated. The spinning cell approach will enable research into the use of liquid crystal lasers in fluorescence imaging and display applications.

1. Introduction

Chiral liquid crystal (CLC) materials can be used to form tunable wavelength microlasers, which have attracted considerable research interest since their inception [1–4]. These devices are small and low-cost due to their self-assembling resonant cavity, and have many potential applications, from laser displays to biomedical imaging techniques such as fluorescence microscopy [5]. The helical CLC structure results in a partial, one-dimensional photonic bandgap (PBG) that reflects circularly polarized light of the same handedness as the helix. This structure can be used as mirrorless resonant cavity and, when doped with a suitable gain medium such as an organic dye, laser emission can occur at the PBG edge. The wavelength of a band-edge laser can be widely tuned by controlling the pitch of the CLC, and the self-assembling nature of the LC resonant cavity means they are simple and cheap to fabricate.

LC laser research has highlighted many of the technology's attractive features: high efficiencies (60%) have been achieved through optimized materials and cell construction [6–9], and a full range of visible wavelengths demonstrated [10]. Fine tuning of the laser wavelength has been achieved with electrical [11,12], mechanical [13,14] and thermal [15,16] methods. Despite these advances, LC laser devices are not widely used or commercially available. One limitation is that the dye-doped CLC (DD-CLC) mixture must be pumped optically with a pulsed laser, and relatively large and expensive Q-switched solid state lasers are currently required. Furthermore, the input pulse energy and frequency must be limited and exceeding these limits results in reduced efficiency or complete cessation of laser emission [17]. At l Hz pump frequency, efficient laser dyes can emit up to 19 μJ/pulse [18]. However, LC lasers are rarely operated above 10 Hz, meaning that the average power output is typically low (< 0.2 mW).

Overcoming these pulse frequency and power limitations would allow the use of LC lasers in a far wider range of applications and would remove some of the perceived barriers to commercialization. For example, imaging techniques using scanning lasers require high pulse

#341736 https://doi.org/10.1364/OE.26.026544
Journal © 2018 Received 9 Aug 2018; revised 10 Sep 2018; accepted 10 Sep 2018; published 26 Sep 2018

Optics EXPRESS

frequencies or continuous-wave operation to achieve acceptable frame rates. Higher average power would also be beneficial for many imaging and display applications.

Experimental studies by Morris et al. concluded that the primary cause of performance degradation at high input power is the distortion of the CLC structure, through optically induced rotation of the LC and dye molecules [19]. This was accompanied by a redshift in emission wavelength. The rotation of the molecules results in degradation of the resonant cavity and ultimately the cavity losses become too large for laser emission. A local rise in temperature caused by high power illumination contributes to distortion of the CLC structure [20]. Etxebarria *et al.* argued that thermal effects also increase scattering of the pump beam, which significantly reduces laser efficiency [21]. Polymer stabilization of the CLC may provide a mechanism for improved resistance to optically and thermally induced LC reorientation [14,22], but introduce increased difficulties in achieving high quality LC alignment and thus efficient, low-threshold and narrow-linewidth laser emission.

Furthermore, the response of the dye molecules to the pump laser pulses influences the maximum input pulse frequency and energy that can be used. Lasing transitions occur between two singlet states in the laser dye, and are prohibited from triplet states. Organic dyes are prone to energy transfer to triplet states when a high pulse energy, long pulse duration or high pulse frequency is used, resulting in a temporary loss in efficiency until triplet states have recovered. With extremely high input energies it is also possible to permanently damage the dye molecules, further reducing the efficiency of the LC laser system [23]. Photostability is therefore a major consideration when selecting suitable laser dyes.

Alternative gain media, such as fluorescent inorganic nanoparticles or quantum dots, are being investigated as a route to higher average power operation [24] but these are often insoluble in the LC host so can aggregate, preventing efficient absorption of the pump laser and distorting the LC structure [25]. Quantum dots typically have a lower quantum efficiency than organic dyes, and have not yet resulted in low threshold, high efficiency lasing, when compared to DD-CLC lasers [24].

Another approach that allows pumping with high energy pulses is to use more of the available gain medium in a DD-CLC cell, by distributing the pump energy through a microlens array and re-combining the output from the resulting array of LC lasers [26]. However, this method does not improve performance at high repetition rates.

Methods that improve the repetition rate and stability of DD-CLC lasers by moving the pump laser relative to the DD-CLC mixture have also been reported. Computer generated holographic pumping was used to dynamically direct each pump spot (or array or spots) to a different area of the LC cell [27], allowing operation at 600 Hz pump frequency, but with undesirable displacement of the output beam. Flowing the DD-CLC material [28]— a method commonly used in commercial dye lasers to reduce thermal effects [29]— allowed use of a 1 kHz pump but resulted in wavelength changes and will also have an upper flow rate limit where the CLC structure is destroyed through flow-induced alignment processes. Slow rotation of a LC laser cell has been shown to be advantageous in improving the stability of the laser emission over several hours at low repetition rates [30]. However, the authors did not investigate the potential for this principle to be used to achieve high repetition rate operation. Rotating discs have also been used to achieve continuous wave emission in solid-state dye lasers [31].

This paper reports a high efficiency LC laser system that can operate at up to 10 kHz pump frequency by rapidly rotating the cell. The stability of the laser emission energy and wavelength is investigated. Operation methods to achieve maximum average power output from the system are discussed and the application of this technique towards simple and fast wavelength-switching is demonstrated.

Optics EXPRESS

2. Experimental setup

2.1 LC laser cell fabrication

Chiral nematic LC mixtures (Table 1) were fabricated from the nematic mixture BL006 (Merck) and the high twisting power chiral dopant BDH1281 (Merck). A laser dye, either pyrromethene 597 (PM597, Exciton) or pyrromethene 650 (PM650, Exciton), was then added.

Four reflective cells were fabricated in-house, each consisting of a pair of 15 mm × 15 mm × 3 mm glass substrates, with a minimum flatness of 4λ (OptoSigma), one of which was mirrored. The substrates were spin-coated with a polyimide alignment layer (SE1410, Nissan Chemical Industries) and anti-parallel rubbed to promote planar LC alignment. The cell gap was controlled at the edges with 10 μm diameter silica spheres (Sinochem Nanjing Corporation) in Norland Optical Adhesive 68 (Thorlabs) at 2%wt. The cells were capillary filled with a laser mixture at 100°C and cooled on a hotplate to 30°C at 0.3°C/min. The edges were sealed with Torr Seal epoxy adhesive (Agilent Technologies).

Table 1. The composition of the LC laser mixture in each of the four cells.

Cell	Mixture	Chiral dopant concentration ($\%_{wt}$)	Dye material	Dye concentration ($\%_{wt}$)
A B	1	4.22 ± 0.07	PM 597	0.7 ± 0.1
C	2	3.87 ± 0.07	PM 650	0.6 ± 0.1
D	3	3.77 ± 0.07	PM 650	1.0 ± 0.1

2.2 Optical and mechanical setup

A 532 nm passively Q-switched diode pumped solid state Nd:YAG laser (Crylas FDSS 532-Q2) was used as the pump, as shown in Fig. 1. The linearly polarized pulsed beam (maximum pulse frequency 10 kHz, FWHM ≤ 1.3 ns) was passed through a rotatable half wave plate and Glan laser linear polarizer to allow attenuation of the pulse energy. The beam was then passed through a quarter wave plate, aligned so as to circularly polarize the beam with the opposite handedness to the CLC, preventing reflection of the pump by the PBG. The pump beam was expanded to better fill a lens with a 25.4 mm aperture, was reflected by a 550 nm cut-off dichroic mirror and focused onto the LC laser cell with an achromatic lens. This resulted in a 90° pump angle and a spot diameter of D_{spot} = 100 μm (measured using the knife-edge method [32]).

The LC laser cell was mounted on an aluminum spinning disk, controlled by a stepper motor with a step-angle of θ = 0.72°, resulting in 500 steps per rotation. The motor was mounted on a translation stage such that the pump spot could be offset from the axis of rotation. This ensured that the pump beam was incident on the cell along the circumference of a circle of known diameter (the 'pump ring'). The laser light emitted from the cell (in a diverging cone normal to the substrates) passed through the achromatic lens and dichroic mirror, and was focused through a long pass edge filter (550 nm) either towards an energy meter (Ophir PD10) or a spectrometer (Ocean Optics USB4000).

Optics EXPRESS

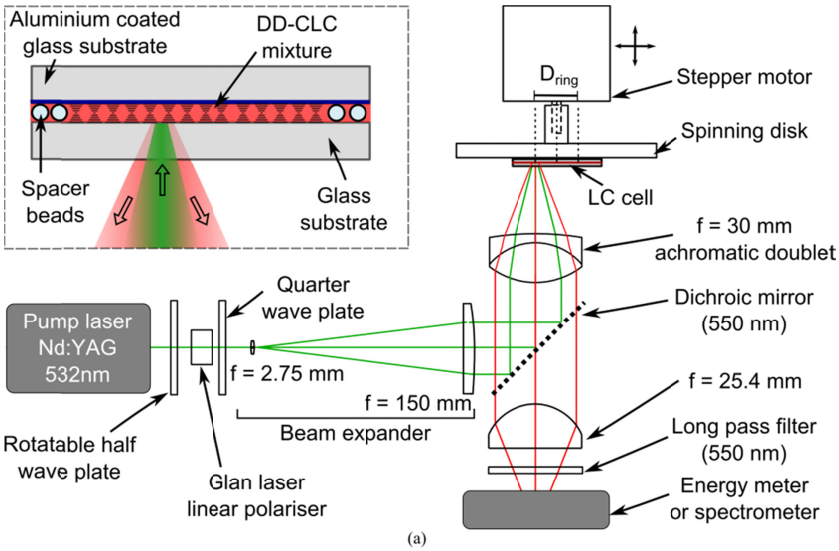

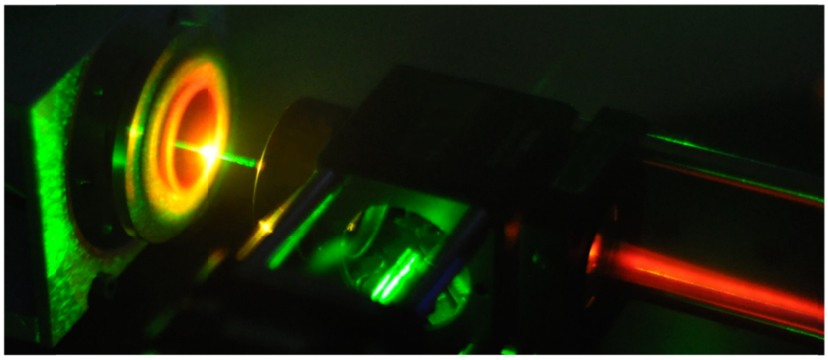

(b)

Fig. 1. (a) The optical arrangement for lasing. A cross-section of a LC laser cell is illustrated in the inset (top left) and shows the focused pump laser beam (green) and diverging LC laser emission (red). (b) A photograph of a spinning cell with a green pump and red emission.

2.3 Experimental method

Three different input pulse energies were used: E_1 = (0.53 ± 0.04) μJ/pulse, E_2 = (2.8 ± 0.6) μJ/pulse, E_3 = (4.9 ± 0.1) μJ/pulse. In spinning cell experiments, the motor was operated at a step frequency equal to the pump laser pulse frequency to ensure a new location for each pump pulse.

Cells A and B (prepared identically and filled with mixture 1) were used to compare the output of a static cell to the spinning system, with pump pulse energy E_1 and a pump ring diameter, D_{ring} = 3 mm. This pump ring was contained entirely within the area of the cell. Emission energy data representative of a larger pump ring diameter (D_{ring} = 20 mm) was collected by positioning the cell over an arc of the pump ring. In static cell experiments, each set of measurements was made using an unused area of the cell to avoid potential cumulative damage. For spinning cell experiments, the same area of the cell was used (as cumulative damage was not expected) but the lowest pump frequencies measured first. The cell was covered for approximately 10 s between measurements at different pump frequencies, to allow some heat dissipation and recovery of any triplet states. The system was also left running for several hours to gain insight into the longer term stability of the system. The maximum average power output possible with this system was also explored by repeating the

Optics EXPRESS

spinning cell experiments with pump pulse energies E_2 and E_3. Cell C was used to study the emission spectra of a spinning cell system and investigate the effect of increasing the pump ring diameter. Cells B, C and D were then secured to the spinning disk together to demonstrate a 3-colour switching laser system.

The slope efficiencies of static and spinning cells were measured using the following methods. The mean output energy from static cells was recorded over a period of 10 s. The mean output energy from spinning cells, at motor step frequencies of 10 Hz and 10 kHz, was recorded over 1 full rotation (50 s) and 100 rotations (5 s), respectively.

3. Results and discussion

As expected, the emission from a static LC laser cell (lowest input pulse energy, E_1) was not stable at pump frequencies above 100 Hz, whereby a significant decrease in output energy per pulse was seen in the first 60 s. Higher pump frequencies resulted in faster reduction of output energy, as shown in Fig. 2(a). This reduction is likely due to a combination of optically induced distortions to the DD-CLC structure and cumulative thermal effects, as discussed in Section I. The triplet state lifetime of PM597 is ~0.1 ms, suggesting that accumulation of triplet states would not be significant using our pump laser which delivers 1.3 ns pulses below 10 kHz [33,34].

The emission energy from a spinning cell is shown in Fig. 2(b). In contrast to the static cell results, the output energy per pulse was constant over 60 s with all pump frequencies used. The spinning system was thus successful in allowing operation of a LC laser at 10 kHz as demonstrated in Visualization 1. Over a 60 s period, the cumulative effects of operating the laser system at the upper end of the range of available pump frequencies were negligible using this pulse energy (E_1). The maximum pump frequency that could be used while maintaining stable emission over 60 s could not be established due to the limitations of the pump laser.

The efficiency of a static cell at low pump frequency (10 Hz,) was found to be 12% and is compared to the same cell spinning with step rates of 10 Hz and 10 kHz in Fig. 2(c). As expected, we observed similar efficiency results at all spin speeds. Lasing thresholds were below the limit of detection, but are less than 89 nJ/pulse (1.1 mJ/cm^2).

Optics EXPRESS

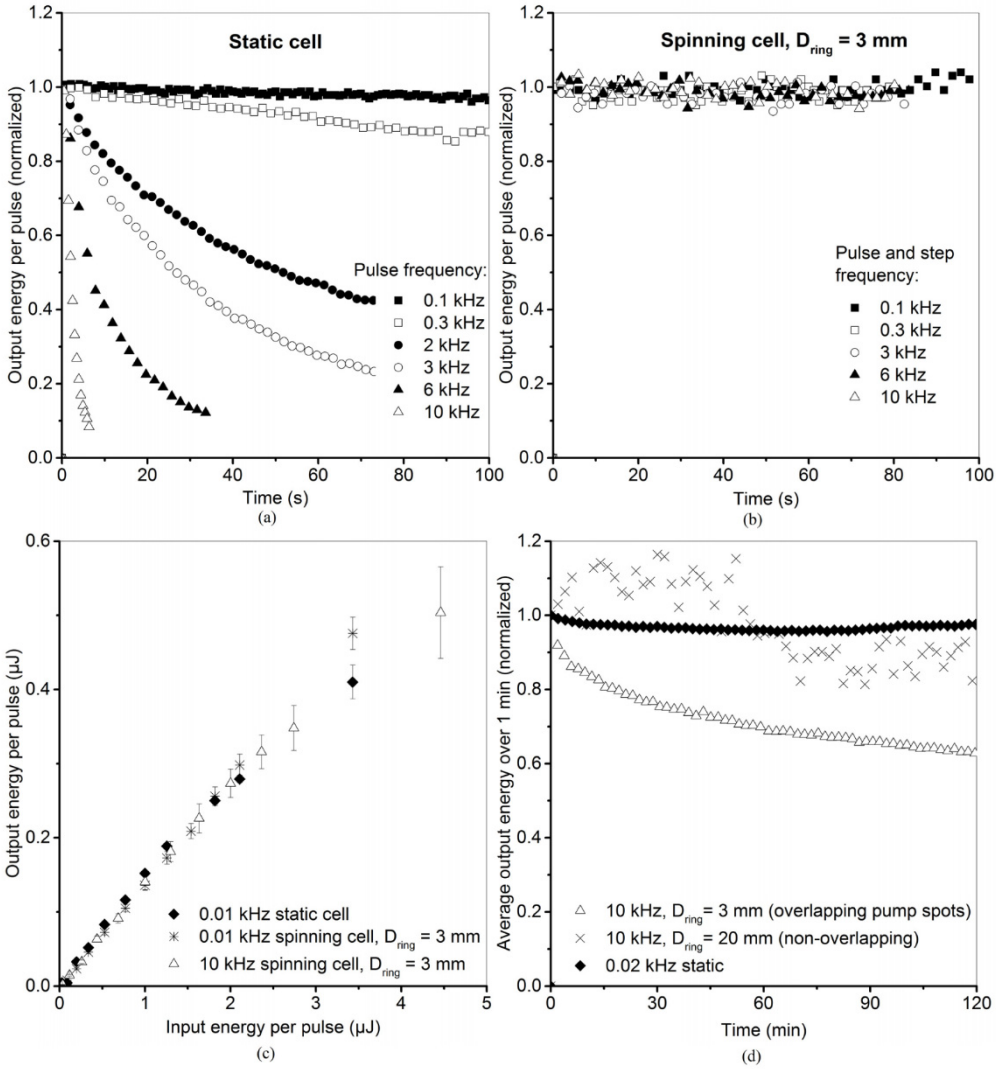

Fig. 2. A comparison between the emission from cell A (a) when static and (b) when spinning, with different pump pulse frequencies, input energy E_I and D_{ring} = 3 mm. The emission energy was normalized to the mean of the first ten data points recorded and down-sampled before plotting for clarity. (c) The slope efficiency when static compared to slowly spinning and spinning at 10 kHz (D_{ring} = 3 mm). Error bars show the standard deviation on the mean energy output. Note that spinning the cell had no detrimental effect on its efficiency. (d) Emission from cell B at 10 kHz over 2 hours for two different pump ring diameters. In the case of non-overlapping pump spots, the data show similar stability to a static cell at 0.02 kHz (i.e. the same effective pump frequency).

The stability of the LC laser when operated at 10 kHz was then investigated by running the system for 2 hours and recording the mean energy per pulse over each 1 s period. The results, plotted in Fig. 2(d), show that the laser was still operating effectively after 2 hours, but with approximately 65% of the original output energy per pulse. In the case of this 3 mm pump ring, consecutive pulses were overlapping, which is likely to have exacerbated optical and thermal distortions to the CLC structure. It was hypothesized that the long term stability at 10 kHz could be improved by increasing the pump ring diameter to prevent consecutive pump spots from overlapping, as illustrated in Fig. 3. Results from an experiment using a larger pump ring diameter (D_{ring} = 20 mm) are included in Fig. 2(d), and show a small

Optics EXPRESS

improvement in stability: the output energy per pulse was still at approximately 85% of the original output after 2 hours of operation at 10 kHz. Theoretically, each spot in this large diameter pump ring is subjected to an 'effective pump frequency' of 20 Hz (pump frequency / number of spots) and thus should be equivalent the behavior of a static cell system at 20 Hz. The output energy from a static cell at 20 Hz remained within 96% of the original output after 2 hours (see Fig. 2(d)), close to the stability of the spinning cell with equivalent effective pump frequency.

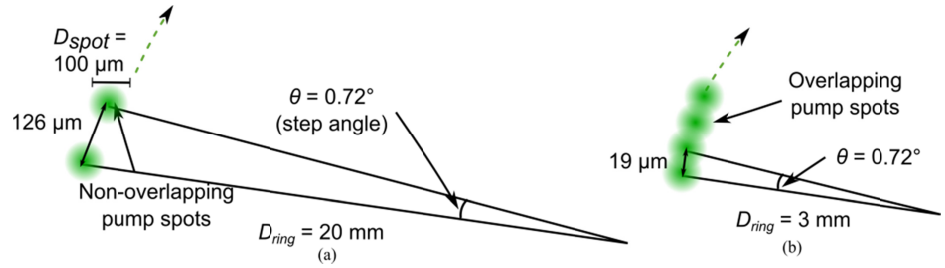

Fig. 3. (a) Illustration of a pump ring with diameter large enough to prevent consecutive pump spots from overlapping. (b) A smaller pump ring with overlapping pump spots.

The use of larger pump ring diameters had the side-effect of increasing the variation in output energy from pulse to pulse, due to variations in the imperfect polydomain CLC structure across the cell. These different chiral domains also affected the wavelength of the emitted laser light. The emission spectrum of a single spot (peak at 662.7 nm) is compared to the sum of all 500 spots in a pump ring in Fig. 4. A small pump ring (3 mm) resulted in a slight broadening of the laser line, from a FWHM of approximately 0.9 nm to 2.4 nm. Larger pump ring diameters cause the excitation of multiple chiral domains of spatially-varying pitch lengths, resulting in a greater variation in emission wavelengths and increased linewidth. The emergence of a second laser peak of shorter wavelength (651.2 nm) is thought to be due to a half-integer increase in the number of chiral pitches present between the substrates, which would theoretically result in an 11.5 nm wavelength reduction. Narrower linewidth emission (0.13 nm) has previously been achieved with a LC laser [5], indicating that with improvements to cell fabrication techniques leading to larger chiral monodomains there is potential to further optimize this parameter.

Optics EXPRESS

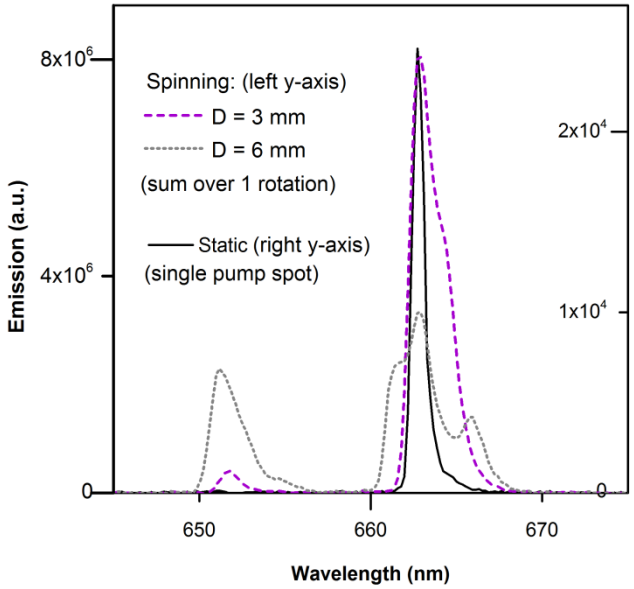

Fig. 4. An emission spectra from a static LC cell (black, solid line) and the sum of all 500 emission spectra recorded during a single rotation of the spinning LC cell system at D_{ring} = 3 mm (purple, short-dash line) and D_{ring} = 6 mm (grey, long-dash line).

It may be possible to increase CLC domain sizes through greater control of the cell fabrication process, reducing both wavelength and energy variations. This may be achievable with further process development in an optimized commercial facility, and would allow the use of larger pump rings in combination with smaller step angles in order to increase the number of pulses per rotation without consecutive pump spots overlapping. For example, pumping at 100 kHz whilst maintaining an effective pump frequency at each spot of 20 Hz would be possible with an 8 cm diameter cell. There is clearly a limit to this approach, due to the size of equipment; a 1 MHz pump frequency would require an impractical 1 m diameter cell. Alternative solutions to managing thermal effects would therefore be required to achieve megahertz pulse frequencies. One possible approach is to stabilize the CLC structure to reduce distortion, for example with polymerization [14,22].

The highest average power recorded for a spinning LC laser with a small wavelength variation (D_{ring} = 3 mm) was 3.5 mW. This was achieved by increasing the input pump energy to E_3, as shown in Fig. 5. However, when using a high pulse energy, the highest pump frequencies were no longer stable over a period of 60 s, as indicated by the large error bars on some high energy data points. This result agrees with the trends shown by Morris *et al.* [19], and shows that effect of increasing pulse energy is similar with the relatively low pulse energies used in our spinning cell experiments. It should be noted that high pulse energies resulted in some permanent degradation of cell performance, although the damage may have been exacerbated by LC mixture leaking from the cell. The most effective strategy for achieving high average power output that is stable over 60 s or longer therefore appears to be to use a low pulse energy with a much higher pump frequency. With the 8 cm diameter cell discussed previously, allowing pump frequencies of 100 kHz, output power in excess of 10 mW would be possible with pump energy E_1, assuming a similar cell efficiency. Higher pulse energies could clearly be used to achieve much higher average power if a shorter period of stable emission was acceptable.

Optics EXPRESS

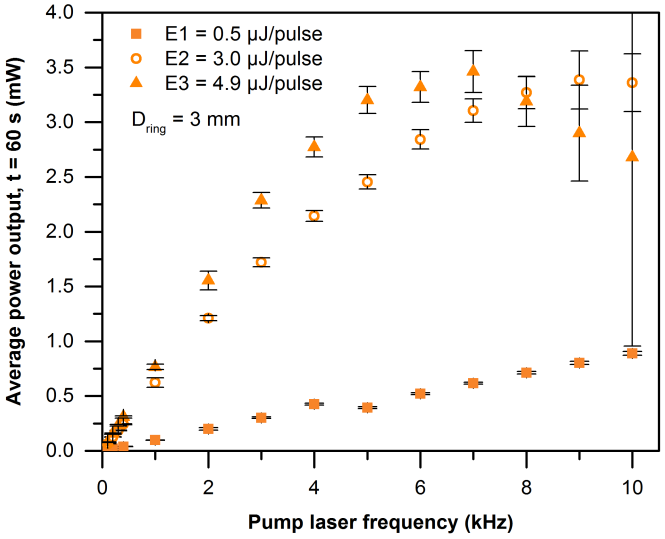

Fig. 5. The average power output of cell A with different pump frequencies, over a period of 60 s. Results from experiments with input pulse energies are shown (E_1 = squares, E_2 = circles, E_3 = triangles). Error bars show the standard deviation in the output power over this period. The use of high energy input pulses was seen to damage the cell. A maximum average power of 3.5 mW was recorded.

The spinning cell system can also be used as a wavelength switching mechanism, by passing the pump beam over a pre-selected sequence of LC laser mixtures. This method is demonstrated in Fig. 6, where a pump frequency and stepper motor frequency of 10 Hz was used to switch the pump laser between 3 different LC laser cells. The emission energy per pulse was lower for cells C and D due to their lower slope efficiencies (4% and 5% respectively), caused primarily by the misalignment of the absorption spectrum of the PM650 dye used in these cells with the 532 nm pump wavelength. The number of pulses of each wavelength is determined by the size of the active area of the cell and the step angle; in the example shown, more pump pulses are incident on cell B than on the other cells, hence that cell's wavelength is emitted for longer. The wavelength variation using cell B is greater than seen from the cells with smaller active area, due to variations in the CLC structure over large areas. The shape and position of the cells could be designed to minimize 'dead time' between cells and enable faster switching. Cell shape and size could also be used control the number of wavelengths and their relative emission durations.

Although demonstrated at a low pump frequency, this approach is equally effective at high pump frequencies and could therefore allow high frequency wavelength switching, as demonstrated in Visualization 1. The technique provides a simple, low-cost solution for pre-programmed laser wavelength sequences in the visible spectrum.

Optics EXPRESS

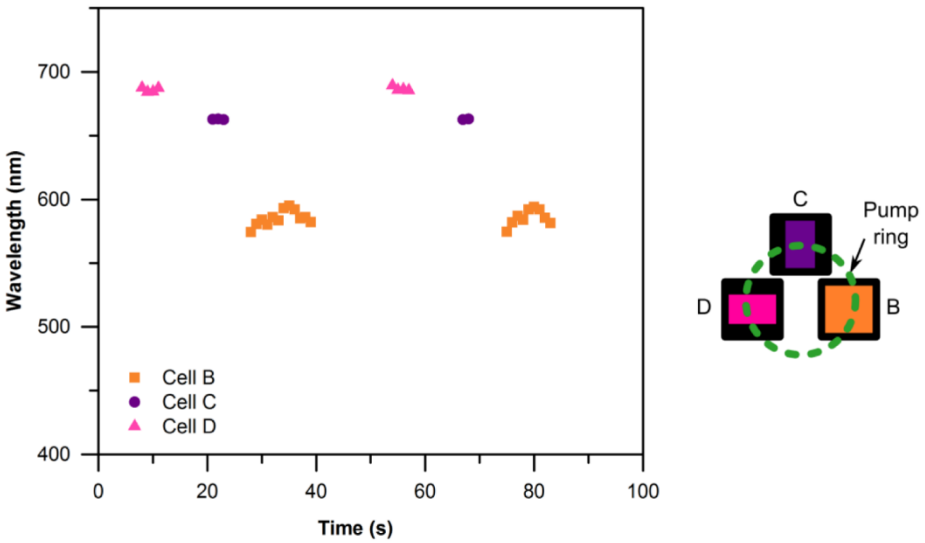

Fig. 6. A demonstration of a wavelength switching technique using 3 cells (B = orange square, C = purple circle and D = pink triangle) mounted on the spinning disk. The cells had different active areas, resulting in slightly different output characteristics. A diagram of the path of the pump ring over the cells shown to the right of the graph.

4. Conclusions

The spinning cell technique outlined in this paper has enabled higher repetition rate operation of a LC laser. This approach can also enable stable operation at higher average power, with the optimum combination of pulse energy and frequency. The improved output opens up opportunities to use LC laser technology in imaging and display applications that would benefit from capabilities such as wavelength tuning or pre-programmed wavelength sequences, with low cost, compact equipment.

Further average power and repetition rate improvements are likely to be possible by using this approach with a pump laser that can deliver much higher repetition rates. Highly controlled cell fabrication methods that minimize wavelength variation will be crucial in the successful use of this technique with larger pump rings.

Funding

MCN was supported by the Engineering & Physical Sciences Research Council (EPSRC) Centre for Doctoral Training in Intelligent Sensing and Measurement; grant number EP/L016753/1. CC was supported by the Scottish Funding Council (SFC) Follow-On Innovation Voucher Scheme. The work was also supported by an EPSRC Impact Acceleration Award; grant number EP/K503794/1. In accordance with funding requirements, data from this research can be accessed at http://dx.doi.org/10.7488/ds/2407.

Acknowledgments

The authors would like to thank A. Mullen of the School of Engineering Mechanical Workshop (University of Edinburgh) for his assistance with the construction of the spinning cell system.

References

1. I. P. Ilchishin, E. A. Tikhonov, V. G. Tishchenko, and M. T. Shpak, "Generation of a tunable radiation by impurity cholesteric liquid crystals," Lett. J. Exp. Theor. Phys. **32**, 24–27 (1980).
2. J. P. Dowling, M. Scalora, M. J. Bloemer, and C. M. Bowden, "The photonic band edge laser: A new approach to gain enhancement," J. Appl. Phys. **75**(4), 1896–1899 (1994).

Optics EXPRESS

3. V. I. Kopp, B. Fan, H. K. M. Vithana, and A. Z. Genack, "Low-threshold lasing at the edge of a photonic stop band in cholesteric liquid crystals," Opt. Lett. **23**(21), 1707–1709 (1998).
4. P. Porov, V. S. Chandel, and R. Manohar, "Lasing characteristics of dye-doped cholesteric liquid crystal," Trans. Electr. Electron. Mater. **16**(3), 117–123 (2015).
5. H. Coles and S. Morris, "Liquid-crystal lasers," Nat. Photonics **4**(10), 676–685 (2010).
6. C. Mowatt, S. M. Morris, T. D. Wilkinson, and H. J. Coles, "High slope efficiency liquid crystal lasers," Appl. Phys. Lett. **97**(25), 251109 (2010).
7. F. Araoka and H. Takezoe, "Towards highly-efficient liquid crystal microlasers," Proc. SPIE **7935**, 79350A (2011).
8. G. Sanz-Enguita, J. Ortega, C. L. Folcia, I. Aramburu, and J. Etxebarria, "Role of the sample thickness on the performance of cholesteric liquid crystal lasers: Experimental, numerical, and analytical results," J. Appl. Phys. **119**(7), 073102 (2016).
9. S. M. Morris, A. D. Ford, M. N. Pivnenko, O. Hadeler, and H. J. Coles, "Correlations between the performance characteristics of a liquid crystal laser and the macroscopic material properties," Phys. Rev. E Stat. Nonlin. Soft Matter Phys. **74**(6), 061709 (2006).
10. P. J. W. Hands, C. A. Dobson, S. M. Morris, M. M. Qasim, D. J. Gardiner, T. D. Wilkinson, and H. J. Coles, ""Wavelength-tuneable liquid crystal lasers from the visible to the near-infrared," Proc. SPIE 8114," Liq. Cryst. **XV**, 81140T (2011).
11. J. Schmidtke, G. Jünnemann, S. Keuker-Baumann, and H. Kitzerow, "Electrical fine tuning of liquid crystal lasers," Appl. Phys. Lett. **101**(5), 051117 (2012).
12. C. T. Wang, C. W. Chen, T. H. Yang, I. Nys, C. C. Li, T. H. Lin, K. Neyts, and J. Beeckman, "Electrically assisted bandedge mode selection of photonic crystal lasing in chiral nematic liquid crystals," Appl. Phys. Lett. **112**(4), 043301 (2018).
13. H. Finkelmann, S. T. Kim, A. Muñoz, P. Palffy-Muhoray, and B. Taheri, "Tunable mirrorless lasing in cholesteric liquid crystalline elastomers," Adv. Mater. **13**(14), 1069–1072 (2001).
14. S. M. Wood, F. Castles, S. Elston, and S. M. Morris, "Wavelength tuneable laser emission from stretchable chiral nematic liquid crystal gels via in-situ photopolymerization," RSC Advances **6**(38), 31919–31924 (2016).
15. K. Funamoto, M. Ozaki, and K. Yoshino, "Discontinuous Shift of Lasing Wavelength with Temperature in Cholesteric Liquid Crystal," Japanese J. Appl. Physics, Part 2 Lett **42**, 7–10 (2003).
16. Y. Huang, Y. Zhou, C. Doyle, and S.-T. Wu, "Tuning the photonic band gap in cholesteric liquid crystals by temperature-dependent dopant solubility," Opt. Express **14**(3), 1236–1242 (2006).
17. S. M. Morris, A. D. Ford, C. Gillespie, M. N. Pivnenko, O. Hadeler, and H. J. Coles, "The emission characteristics of liquid-crystal lasers," J. Soc. Inf. Disp. **14**(6), 565–573 (2006).
18. C. Mowatt, S. M. Morris, M. H. Song, T. D. Wilkinson, R. H. Friend, and H. J. Coles, "Comparison of the performance of photonic band-edge liquid crystal lasers using different dyes as the gain medium," J. Appl. Phys. **107**(4), 043101 (2010).
19. S. M. Morris, A. D. Ford, M. N. Pivnenko, and H. J. Coles, "The effects of reorientation on the emission properties of a photonic band edge liquid crystal laser," J. Opt. A, Pure Appl. Opt. **7**(5), 215–223 (2005).
20. A. Varanytsia and P. Palffy-Muhoray, "Thermal degradation of the distributed-feedback cavity in cholesteric liquid crystal lasers," Proc. SPIE 8828. Liq. Cryst. **XVII**, 88281F (2013).
21. J. Etxebarria, J. Ortega, C. L. Folcia, G. Sanz-Enguita, and I. Aramburu, "Thermally induced light-scattering effects as responsible for the degradation of cholesteric liquid crystal lasers," Opt. Lett. **40**(7), 1262–1265 (2015).
22. A. Muñoz, M. E. McConney, T. Kosa, P. Luchette, L. Sukhomlinova, T. J. White, T. J. Bunning, and B. Taheri, "Continuous wave mirrorless lasing in cholesteric liquid crystals with a pitch gradient across the cell gap," Opt. Lett. **37**(14), 2904–2906 (2012).
23. C. V. Shank, "Physics of dye lasers," Rev. Mod. Phys. **47**(3), 649–657 (1975).
24. L.-J. Chen, J.-D. Lin, and C.-R. Lee, "An optically stable and tunable quantum dot nanocrystal-embedded cholesteric liquid crystal composite laser," J. Mater. Chem. C Mater. Opt. Electron. Devices **2**(22), 4388–4394 (2014).
25. A. L. Rodarte, Z. S. Nuno, B. H. Cao, R. J. Pandolfi, M. T. Quint, S. Ghosh, J. E. Hein, and L. S. Hirst, "Tuning quantum-dot organization in liquid crystals for robust photonic applications," ChemPhysChem **15**(7), 1413–1421 (2014).
26. P. J. W. Hands, S. M. Morris, T. D. Wilkinson, and H. J. Coles, "Two-dimensional liquid crystal laser array," Opt. Lett. **33**(5), 515–517 (2008).
27. S. M. Wood, T. K. Mavrogordatos, S. M. Morris, P. J. W. Hands, F. Castles, D. J. Gardiner, K. L. Atkinson, H. J. Coles, and T. D. Wilkinson, "Adaptive holographic pumping of thin-film organic lasers," Opt. Lett. **38**(21), 4483–4486 (2013).
28. T. Dadalyan, R. Alaverdyan, I. Nys, Z. Ninoyan, O. Willekens, J. Beeckman, and K. Neyts, "Tuning the lasing wavelength of dye-doped chiral nematic liquid crystal by fluid flow," Liq. Cryst. **8292**, 1–7 (2016).
29. G. K. Mishra, A. Kumar, S. K. Sharma, A. J. Singh, O. Prakash, P. K. Mukhopadhyay, K. S. Bindra, S. K. Dixit, and S. V. Nakhe, "Study of output power of very high pulse repetition rate (18 kHz) dye laser pumped by frequency doubled diode pumped Nd: YAG laser ($\lambda \sim 532$ nm)," Laser Phys. **25**(5), 055001 (2015).
30. G. Chilaya, A. Chanishvili, G. Petriashvili, R. Barberi, M. P. De Santo, and M. A. Matranga, "Enhancing cholesteric liquid crystal laser stability by cell rotation," Opt. Express **14**(21), 9939–9943 (2006).

Optics EXPRESS

31. R. Bornemann, U. Lemmer, and E. Thiel, "Continuous-wave solid-state dye laser," Opt. Lett. **31**(11), 1669–1671 (2006).
32. W. J. Marshall, "Two methods for measuring laser beam diameter," J. Laser Appl. **22**(4), 132–136 (2010).
33. H. A. Montejano, F. Amat-Guerri, A. Costela, I. García-Moreno, M. Liras, and R. Sastre, "Triplet-state spectroscopy of dipyrromethene BF2 laser dyes," J. Photochem. Photobiol. Chem. **181**(2-3), 142–146 (2006).
34. J. Ortega, C. L. Folcia, and J. Etxebarria, "Upgrading the performance of cholesteric liquid crystal lasers: Improvement margins and limitations," Materials (Basel) **11**(1), 5 (2017).